NMR Relaxation Study of the Protonated Form of 1,8-Bis(dimethylamino)naphthalene in Isotropic Solution: Anisotropic Motion outside of Extreme Narrowing and Ultrafast Proton Transfer

Piotr Bernatowicz,† Jozef Kowalewski,* and Dick Sandström

Physical Chemistry, Arrhenius Laboratory, Stockholm University, S-106 91 Stockholm, Sweden

Received: October 6, 2004

The protonated form of 1,8-bis(dimethylamino)naphthalene ($DMANH^+$) consists of a rigid, aromatic framework, substituted by two amino groups that are connected by a strong, symmetric (on the NMR time-scale) hydrogen bond bridge. The reorientational motion of the molecule in dimethylformamide-d7 solution was characterized by T_1 and NOE measurements for aromatic ^{13}C nuclei. Treating the reorientation of $DMANH^+$ as anisotropic rotational diffusion of a rigid body, the diffusion tensor was determined with good accuracy. Measurements and interpretation of ^{15}N T_1 and NOE indicate that the proton transfer between potential minima in the hydrogen bond bridge is faster than the molecular reorientation.

1. Introduction

The title compound, *N*,*N*,*N*′,*N*′-tetramethyl-1,8-naphthalenediamine (DMAN) is often called a "proton sponge" because of its extremely high basicity. Its pK_a (12.1) is about seven units larger compared to other aromatic amines such as, e.g., aniline or 1,8-diaminonaphthalene.[1,2] In a reaction with acids, DMAN absorbs a proton into the space between the nitrogens, where a very strong intramolecular hydrogen bond is formed.[3−5] The act of protonation leads to a remarkable rearrangement of the electron density not only in vicinity of the nitrogen atoms but also in the aromatic rings of the naphthalene fragment.[6] This can be easily deduced, e.g., by observing changes of ^{13}C NMR signal positions, which for ortho and para carbons are shifted by about 10 ppm downfield after protonation, compared to neat amine. More direct insight into the molecular geometry changes provided by neutron scattering methods[6,7] reveals that protonation, apart from slight shortening of C−C bonds and elongation of C(ar)−H bonds, causes substantial elongation of C(ar)−N bonds and change of the N−N distance from 2.804 to 2.644 Å. Moreover, the DMAN molecules, significantly twisted in the crystal, acquire after absorption of a proton C_{2v} symmetry. The [N−H−N] bridge seems to be stable not only in the solid state but also in solution. The latter fact is suggested, e.g., by the existence of a relatively large scalar coupling between the nitrogen nuclei, $^{2h}J(^{15}N-^{15}N) = 8.7$ Hz,[8] which follows with the presence of a proton in the bridge, but would be absent otherwise. Proton-decoupled ^{13}C NMR spectra acquired in solution over a broad temperature range contain only one signal of all the methyl groups and six signals of the naphthalene part.[9,10] This is a manifestation of a high symmetry of the average liquid-state NMR Hamiltonian of $DMANH^+$ (Figure 1), which belongs to the C_{2v} point group. Such a symmetry is not obvious. It may be a consequence of fast proton jumps between double-well potential minima located at both sides of the symmetry plane, σ_v', perpendicular to the plane σ_v of the naphthalene ring, but also a proton localization in the minimum of a single-well potential may not be a priori rejected. In light of neutron scattering results, the latter picture seems to be less probable but, in principle, the interaction with solvent molecules might cause a collapse of the double-well potential into a single minimum. However, the latter model of the potential shape in solvated $DMANH^+$ was in addition found[11,12] inconsistent with the large positive first-order isotope effect, $(\delta_H - \delta_D) = +0.66$. Therefore, we discard the possibility of a proton localization in the middle of the bridge, and interpret our experimental data assuming that the occurrence of seven signals in the $^{13}C\{^1H\}$ NMR spectrum may be explained in terms of proton jumps fast enough to average chemical shift differences of nuclei mutually related by the σ_v' plane.

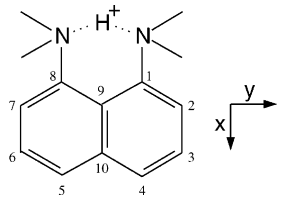

Figure 1. Directions of principal axes of the rotational diffusion tensor in the $DMANH^+$ molecule.

The frequency difference between the ^{15}N NMR signals in the case when the proton is on one side of the double well was estimated in the solid state to be about 7 ppm.[13] At external magnetic fields of magnitudes typical for modern NMR spectrometers, such a small difference would be averaged out at exchange rates much lower than 10^3 Hz, yielding a single nitrogen signal. When the jump rate exceeds $10^4 - 10^5$ Hz, the residual line broadening caused by the exchange becomes smaller than line shape effects introduced, e.g., by magnetic field inhomogeneity. This renders details of the proton dynamics undetectable not only for NMR methods such as exchange spectroscopy (EXSY) but also in analysis of transverse relaxation times, T_2, or longitudinal relaxation times measured in the rotating frame, $T_{1\rho}$. Motions that are faster than 10^5 Hz, but still much slower than 10^8-10^9 Hz, are even more difficult to follow by NMR. Usually, they neither remarkably influence spectral line shapes nor cause measurable contributions to spin

* Corresponding author. E-mail: jk@physc.su.se

† On leave from Institute of Organic Chemistry, Polish Academy of Sciences, Kasprzaka 44/52, 01-224 Warsaw, Poland.

10.1021/jp045454n CCC: $30.25
Published on Web 12/09/2004

relaxation. Their impact on the latter processes is at least certainly masked by effects of molecular tumbling. Similar problems arise for dynamics of rates much faster than the overall molecular reorientation, i.e., 10^{11} Hz and higher − their spectral densities are spread over an extremely wide frequency range, so that components of the latter at particular frequencies relevant for nuclear spin relaxation are negligibly small. This is in contrast to relaxation studies in the solid state, where the absence of overall molecular reorientation makes the fast motions a significant source of relaxation.[14,15] Proton jumps of intermediate frequencies, 10^9-10^{11} Hz, similar to the rates of molecular tumbling, can play an important role for spin relaxation. The separation of the global reorientational motion of the molecule as a whole and the internal motion requires, however, the knowledge of the rotational diffusion tensor of the molecule.

Evaluations of the full rotational diffusion tensor for anisotropic tumblers are relatively common in the extreme narrowing regime[16−19] but are scarce outside of this range.[20] In the first part of this work, we show how standard ^{13}C NMR relaxation investigations of high accuracy, supported by solid-state NMR methods and quantum mechanical computations of NMR parameters at the DFT level, can provide the principal components of the diffusion tensor. In the second part, we turn to ^{15}N, exploit a novel idea concerning deconvolution of interfering motions, and try to draw conclusions concerning the nature of the proton motion within the intramolecular hydrogen bond in $DMANH^+$.

2. Theory

In a molecule undergoing rotational Brownian motions in isotropic liquids, the nuclear spin relaxation is caused by time-dependent interactions with the environment. For spin-1/2 nuclei, such as ^{13}C and ^{15}N (S spins) with their low natural abundances, the most important interactions of this type involve dipole−dipole (DD) couplings with neighboring protons (I spins) and the anisotropic part of the chemical shielding tensor (chemical shielding anisotropy, CSA). The broadband decoupling of protons results in a simple monoexponential spin−lattice relaxation of the S spins, characterized by the rate $(T_{1S})^{-1}$, and in the heteronuclear Overhauser enhancement (NOE) of the S-spin signals. Including the DD and CSA mechanisms, the commonly used expression for the spin−lattice relaxation rate is given by[21]

$$(T_{1S})^{-1} = \frac{1}{20}[6J_{DD}(\omega_S + \omega_I) + 3J_{DD}(\omega_S) + J_{DD}(\omega_S - \omega_I)] + \frac{1}{15}J_{CSA}(\omega_S) \quad (1)$$

while the expression for NOE reads

$$\eta = \frac{1}{20}[6J_{DD}(\omega_S + \omega_I) - J_{DD}(\omega_S - \omega_I)]T_{1S}\frac{\gamma_I}{\gamma_S} \quad (2)$$

The expression

$$\rho_S = \frac{1}{20}[6J_{DD}(\omega_S + \omega_I) - J_{DD}(\omega_S - \omega_I)] \quad (3)$$

occurring on the rhs of eq 2 is called the cross-relaxation rate. The spin−lattice relaxation rate depends on the dipolar and CSA spectral densities, $J_{DD}(\omega)$ and $J_{CSA}(\omega)$, respectively, evaluated at various angular frequencies characterizing the energy levels of the spin system. The NOE depends in addition on the ratio of the magnetogyric ratios, γ, for the two species. The spectral densities can in general be related to the dipolar and CSA interaction strengths and to dynamics. The exact form of the relations depends on the situation. We can differentiate between two cases: reorientation of molecules treated as rigid bodies and more complex rotational dynamics, allowing for internal motions. For the rigid-body case, the situation is rather simple. We can write

$$J_{DD}(\omega) = \xi^2\tilde{J}(\omega) = \left(\frac{\mu_0}{4\pi}\frac{\gamma_I\gamma_S\hbar}{r_{IS}^3}\right)^2\tilde{J}(\omega) \quad (4)$$

$$J_{CSA}(\omega) = (\gamma_S B_0\Delta\sigma)^2\left[\left(1 - \frac{\epsilon_{CSA}}{3}\right)^2\tilde{J}_z(\omega) + \frac{4}{9}\epsilon_{CSA}^2\tilde{J}_x(\omega) - \frac{4}{3}\epsilon_{CSA}\left(1 - \frac{\epsilon_{CSA}}{3}\right)\tilde{J}_{xz}(\omega)\right] \quad (5)$$

Here, ξ is a measure of the dipole−dipole interaction strength and $\tilde{J}(\omega)$ are reduced spectral densities. The indices *x*, *z*, and *xz* appear in cases of CSA tensors lacking axial symmetry (see ref 24 for details). The symbol μ_0 in the dipolar interaction strength is the permeability of vacuum, and r_{IS} is the internuclear distance. The dipolar coupling strength can thus be approximately calculated from internuclear distances obtained from neutron diffraction data. $\Delta\sigma$ and ϵ_{CSA} in eq 5 are called the chemical shielding anisotropy and asymmetry, respectively. Both quantities can be expressed in terms of the principal components σ_{ii} of the shielding tensor:

$$\Delta\sigma = \sigma_{33} - (\sigma_{11} + \sigma_{22})/2 \quad (6)$$

$$\epsilon_{CSA} = 3(\sigma_{11} - \sigma_{22})/2\Delta\sigma \quad (7)$$

where we use the convention $|\sigma_{11}| \le |\sigma_{22}| \le |\sigma_{33}|$. In the case of an axially symmetric CSA tensor, eq 5 reduces to

$$J_{CSA}(\omega) = (\gamma_S B_0\Delta\sigma)^2\tilde{J}(\omega) = \chi^2\tilde{J}(\omega) \quad (8)$$

where χ denotes the CSA interaction strength. The chemical shielding tensors can be determined by solid-state NMR, either in a single crystal, where magnitudes of principal components can be extracted together with the principal axis orientation, or in powders using magic-angle spinning (MAS) techniques, if the information about alignment of the tensors with respect to the molecular skeleton can be dispensed with. Quantum mechanical methods can also be helpful.

Of course, no molecules are "real" rigid bodies but, under certain assumptions, the effects of vibrational motions can be limited to small modifications (scaling) of the interactions strengths.[22,23] We assume that the aromatic ^{13}C nuclei and protons in DMAN can, in that sense, be considered to form a rigid framework. The reduced spectral densities characterize the reorientational dynamics of various molecule-fixed axes. In a general rigid-body case, the reduced spectral densities depend on six parameters: three principal components of the diffusion tensor, D_X, D_Y, D_Z, and three Euler angles specifying the orientation of the principal diffusion frame with respect to an arbitrary molecule-fixed frame (e.g., the principal frame of the moment of inertia tensor).[16] In the notation of Canet[24] (μ,μ' label interfering relaxation mechanisms; θ,φ are polar angles specifying the orientation of the principal axes of the interaction μ

with respect to the diffusion tensor frame), the reduced spectral densities are given by

$$\tilde{J}^{\mu\mu'}(\omega) = \sum_{m=-2}^{2} a_m^{\mu\mu'} \frac{(2/\lambda_m)}{1+\omega^2/\lambda_m^2} \tag{9}$$

where

$$\lambda_0 = 4D_Z + 2D_+$$

$$\lambda_{\pm 1} = D_Z + 5D_+ \pm 3D_-$$

$$\lambda_{\pm 2} = 2D_Z + 4D_+ \pm [4(D_Z - D_+)^2 + 12D_-^2]^{1/2} \tag{10}$$

and

$$a_0^{\mu\mu'} = (3/4)\sin^2\theta_\mu \sin^2\theta_{\mu'} \sin 2\varphi_\mu \sin 2\varphi_{\mu'}$$

$$a_{+1}^{\mu\mu'} = (3/4)\sin 2\theta_\mu \sin 2\theta_{\mu'} \sin\varphi_\mu \sin\varphi_{\mu'}$$

$$a_{-1}^{\mu\mu'} = (3/4)\sin 2\theta_\mu \sin 2\theta_{\mu'} \cos\varphi_\mu \cos\varphi_{\mu'}$$

$$a_{\pm 2}^{\mu\mu'} = \frac{1}{12D_-^2 + d_\pm^2}\{(9D_-^2)\sin^2\theta_\mu \cos 2\varphi_\mu \sin^2\theta_{\mu'} \cos 2\varphi_{\mu'} - (3D_- d_\pm)[\sin^2\theta_\mu \cos 2\varphi_\mu (1/2)(3\cos^2\theta_{\mu'} - 1) + (1/2)(3\cos^2\theta_\mu - 1)\sin^2\theta_{\mu'} \cos 2\varphi_{\mu'}] + (d_\pm)^2(1/2)(3\cos^2\theta_\mu - 1)(1/2)(3\cos^2\theta_{\mu'} - 1) \tag{11}$$

with

$$D_\pm = (D_X \pm D_Y)/2$$

$$d_\pm = 2(D_Z - D_+) \mp [4(D_Z - D_+)^2 + 12D_-^2]^{1/2}$$

We note that if the motions are so fast that the ratios (ω^2/λ^2) are small at all relevant frequencies (extreme narrowing regime), eq 9 simplifies to

$$\tilde{J} = 2\tau_c^{\text{eff}} \tag{12}$$

i.e. the spectral densities become independent of frequency, dipolar relaxation rates become independent of the magnetic field, and the field-dependence of the CSA relaxation is only caused by the interaction strength. The effective correlation time, τ_c^{eff}, describes the reorientation of a molecule-fixed axis and depends on its orientation in the diffusion frame and on the diffusion tensor principal components. In the limit of isotropic rotation of a rigid, sphere-like object, the effective correlation time is equal to the unique rotational correlation time. In the extreme narrowing regime, it is impossible to determine the interaction strengths and the dynamic parameters separately.

If a sufficiently large number of independent relaxation rates are measured in a molecule, then the determination of components of the rotational diffusion tensor and its orientation is possible. For DMANH$^+$, the C_{2v} symmetry of the molecule unequivocally determines directions of the rotational diffusion tensor axes (see Figure 1). We tacitly assume that the motion of the bridging proton does not cause any significant rearrangement of the solvation sphere of the molecule, which might be a significant complication. With six nonequivalent aromatic carbons, we have a sufficient number of relaxation sites to determine the three unknown parameters of the diffusion tensor. We note that all the carbon-proton dipolar interaction principal axes lie in one plane, which makes the dipolar relaxation insufficient to derive D_X, D_Y, D_Z. Fortunately, the CSA mechanism which dominates relaxation of carbons 9 and 10, with its principal axis perpendicular to the ring plane, can resolve this difficulty.[25]

A more complicated situation arises in the presence of internal motions. In the DMANH$^+$ molecule with perdeuterated methyl groups, the longitudinal relaxation of ^{15}N magnetization is to a large extent dominated by the dipole−dipole interaction with the proton of the bridge. If it were localized in the middle of a single-well minimum, then eqs 1 and 2 would apply in a straightforward way. If the proton jumps between two potential minima with a rate λ_i, then its motion within the bridge influences the ^{15}N relaxation and the spectral densities given by eqs 4 and 5 no longer describe such a system.

Starting with the formulation of Hubbard,[26] we have derived the following equation describing, without approximations, the dipolar relaxation in a general case involving two-site local dynamics accompanying totally anisotropic molecular reorientation. The details of the derivation are beyond the scope of this work. This issue will be the subject of a forthcoming paper. The dipolar spectral density in such a case reads

$$J_{DD}(\omega) = \frac{1}{4}\sum_{m=-2}^{2}\left\{[\xi^l\xi^l a_m^{ll} + \xi^l\xi^r a_m^{lr} + \xi^r\xi^l a_m^{rl} + \xi^r\xi^r a_m^{rr}]\frac{(2/\lambda_m)}{1+\omega^2/\lambda_m^2} + [\xi^l\xi^l a_m^{ll} - \xi^l\xi^r a_m^{lr} - \xi^r\xi^l a_m^{rl} + \xi^r\xi^r a_m^{rr}]\frac{(2/\lambda_{mi})}{1+\omega^2/\lambda_{mi}^2}\right\} \tag{13}$$

with ξ^l and ξ^r labeling dipolar couplings of ^{15}N to protons in local and remote positions, respectively, and $\lambda_{mi} = \lambda_m + 2\lambda_i$. One should note the lack of factorization of the spectral densities, $J(\omega)$, into a product of a single interaction strength squared, ξ^2, and reduced spectral densities, $\tilde{J}(\omega)$, which simplifies eq 4 for a rigid body. Equations 1, 2, and 3 are still valid. Using the rotational tumbling of the molecule as a reference, with which we compare the intramolecular rates, we can differentiate between three possible cases:

1. Slow jumps, $\lambda_m \gg \lambda_i$. As discussed in the Introduction, all the available experimental evidence is consistent with a proton motion in DMANH$^+$ being fast on the chemical shift time scale, i.e., faster than about 10^3 s^{-1}. If it remains, at the same time, much slower than the rotational tumbling (λ_m), then the role of the internal motion is to average the nitrogen relaxation rates of the two sites. This becomes obvious when one notes that $\lambda_m \gg \lambda_i$ implies $\lambda_{mi} \approx \lambda_m$, which further leads to the following simplification of eq 13

$$J(\omega) = \frac{1}{2}\sum_{m=-2}^{2}[\xi^l\xi^l a_m^{ll} + \xi^r\xi^r a_m^{rr}]\frac{(2/\lambda_m)}{1+\omega^2/\lambda_m^2} \tag{14}$$

The interpretation of this expression is as follows: on the average, half of the nitrogens would be relaxed by the dipolar interaction, ξ^r, with protons occupying remote position, while the other half would be relaxed by the interaction with the local protons, ξ^l.

2. Rapid jumps, $\lambda_m \ll \lambda_i$. If the jumps occur with a rate constant much larger than the tumbling rate, the proton transfer acts as a fast vibration-like motion, averaging the dipolar

interaction strength itself.[23,27] The condition $\lambda_m \ll \lambda_i$ means that the second term on the rhs of eq 13 can be neglected, which leads to

$$J(\omega) \approx \frac{1}{4}\sum_{m=-2}^{2} [\xi^{l}\xi^{l} a_m^{ll} + \xi^{l}\xi^{r} a_m^{lr} + \xi^{r}\xi^{l} a_m^{rl} + \xi^{r}\xi^{r} a_m^{rr}]\frac{(2/\lambda_m)}{1+\omega^2/\lambda_m^2} \quad (15)$$

$$\approx \sum_{m=-2}^{2}\left(\frac{\xi^{l}+\xi^{r}}{2}\right)^2 a_m \frac{(2/\lambda_m)}{1+\omega^2/\lambda_m^2}$$

where the second approximate equality comes from fact that the nitrogen dipolar interactions with local and remote protons are almost collinear, which renders all the coefficients a_m^{ll}, a_m^{lr}, a_m^{rl}, a_m^{rr} almost equal to each other. In the case of CSA relaxation, one can obtain expressions analogous to eqs 14 and 15 and containing the average of the square of the shielding tensor anisotropy or the square of the average anisotropy itself.

3. Intermediate jumps, $\lambda_m \sim \lambda_i$. Unlike the previous cases, eq 13 cannot be further simplified here, and nitrogen dipolar relaxation is therefore dependent not only on the overall molecular tumbling but also on the behavior of the bridging proton itself. The case of jump motion in this motional regime has been considered for spherical and symmetric top molecules, e.g., by Woessner,[28] Tropp,[29] and Latanowicz,[30] under the assumption of uncorrelated global and local motions. We note that the motions might become correlated if the proton transfer in the hydrogen bond causes significant rearrangement of the solvation sphere of the molecule.

3. Experimental Details

N,*N*,*N*′,*N*′-tetramethyl-1,8-naphthalenediamine was purchased from Fluka and purified by 2-fold recrystallization from pentane at 248 K. Nitrate and perchlorate of $DMANH^+$ were prepared following ref 22 in the paper by Pietrzak et al.[8] The salts were recrystallized from acetonitrile and dried under vacuum for several hours. The nitrate salt was used to prepare a 0.15 M solution in DMF-d7, which was afterward sealed in a 5 mm NMR sample tube under an atmosphere of inert gas. All the solution state ^{13}C NMR measurements described in this article were performed on this sample, while all the ^{15}N NMR measurements were performed on the analogous sample of *N*,*N*,*N*′,*N*′-tetramethyl-d12-1,8-naphthalenediamine with isotopic enrichment of 99% of deuterium. This deuterated analogue of $DMANH^+$ was prepared following the procedure of Quast et al.[31] 1,8-Diaminonaphthalene used in the synthesis was purchased from Fluka, while dimethyl-d6-sulfate (99 atom % D) was obtained from Acros Organics. The deuteration of the methyl groups is not expected to influence the ^{13}C relaxation rates of the aromatic carbons. To confirm this assumption, the spin−lattice relaxation rates measured at two different temperatures were compared for the two samples and the consistency was better than 2%.

The ^{13}C and ^{15}N relaxation rates were measured at three magnetic fields, 14.1, 11.7, and 9.4 T, at temperatures of 323, 303, 293, 283, 273, 263, 243, 228, and 213 K, using Varian Unity Inova 600 MHz, Bruker Avance DRX 500 MHz, and Bruker Avance DRX 400 MHz spectrometers. The direct proton-decoupled carbon-detected, fast inversion−recovery experiments[32] were performed for ^{13}C. Typical parameters were as follows: 64 scans for each of the 16 incremented delays, spectral widths between 110 and 135 ppm, acquisition times between 1.5 and 2.5 s, and 90° pulses between 7 and 10 μs. The *Z*-gradient version of indirect detection experiments[33] was applied for ^{15}N. Typical parameters were as follows: 16 scans for each of the 16 incremented delays, spectral widths about 5 ppm, acquisition times about 0.5 s, and 90° pulses 10−12 (30−40) μs for $^1H(^{15}N)$. For the ^{13}C case, the recycle delay was always longer than two times the longest T_1, while for ^{15}N measurements it was longer than five times the T_1 of the bridging proton, which was used for the polarization transfer. For the ^{15}N isotope, also the NOE from the bridging proton was measured at a field of 9.4 T in the same temperature range, using indirect detection,[33] with a recycle delay longer than ten times ^{15}N T_1. The NOE for ^{13}C was measured at a field of 11.7 T with standard procedures based on comparison of intensities in ^{13}C spectra acquired with and without broadband (Waltz modulation) preirradiation of the ^1H frequency. All the experiments were repeated at least twice. We judge the overall accuracy of the measured spin−lattice relaxation rates to be 3−5%, while the accuracy of the NOE factor, $(1 + \eta)$, is better than 0.1 unit.

All spectrometers were equipped with variable temperature units allowing for temperature control with an accuracy of 0.1 K. Temperature calibration was carefully performed using methanol[34] within the range 303−213 K and ethylene glycol[35] at 323 K, respectively. Both the gas flow and decoupling power were also carefully controlled,[36] in order to diminish temperature gradients in the sample. Spectrometers were stabilized for at least 2 h before the measurements were commenced.

Components of the rotational diffusion tensor of $DMANH^+$ in the whole temperature range of interest were obtained from a least-squares iterative analysis of the relaxation and NOE data, which was performed using a Fortran routine, based on the Newton−Raphson algorithm, written in-house.

The ^{13}C chemical shielding tensors needed for the relaxation analysis were obtained from solid-state experiments performed on a solid DMAN perchlorate at a field of 9.4 T on a Chemagnetics Infinity 400 MHz spectrometer, using a 6 mm double-resonance MAS probe. The ^1H decoupling field strength corresponded to a nutation frequency of 75 kHz. The recycle delay and $^1H-^{13}C$ cross-polarization (CP) contact time were 4 s and 3 ms, respectively. The mass of the powder sample for the solid-state NMR experiments was approximately 150 mg. The principal elements of the ^{13}C chemical shielding tensors were determined from spinning-sideband intensities using the

TABLE 1: Experimental ^{13}C Chemical Shielding Tensors[a]

atom number	σ_{11} [ppm]	σ_{22} [ppm]	σ_{33} [ppm]	θ_{33}, φ_{33}[b] [deg]	θ_{11}, φ_{11} [deg]
1,8[c]	4 ± 1	80 ± 3	−84 ± 3	3, 8	91, 25
10	69 ± 3	70 ± 3	−139 ± 6	0, −	−, −
4,5	11 ± 2	96 ± 4	−107 ± 3	0, −	90, 99
3,6	17 ± 3	102 ± 1	−119 ± 3	0, −	90, 143
2,7	21 ± 1	94 ± 1	−115 ± 2	0, −	90, 39
9	59 ± 7	66 ± 4	−125 ± 5	0, −	−, −
CH_3[c,d]	17.9 ± 0.4	19.2 ± 0.7	−37.1 ± 0.8	−, −	−, −
	17.8 ± 0.6	18.7 ± 0.9	−36.5 ± 0.9	−, −	−, −

[a] The principal components were extracted from solid-state MAS measurements of DMAN perchlorate powder. The polar angles with respect to the rotational diffusion tensor reference frame were calculated on the DFT level. Standard errors are given. [b] θ denotes the polar angle with respect to the *Z* axis of rotational diffusion tensor, while φ denotes the azimuthal angle with respect to the *X* axis of this tensor. [c] Relaxation rates of these nuclei were neglected in the course of rotational diffusion tensor estimation. [d] There are two resonances from methyl carbons in the solid state.

TABLE 2: Rotational Diffusion Tensor Components D_X, D_Y, D_Z and One-bond Dipolar Couplings Delivered by the Newton−Raphson Fitting Routine[a]

T [K]	$D_X[10^9 s^{-1}]$	$D_Y[10^9 s^{-1}]$	$D_Z[10^9 s^{-1}]$	ξ_{C2} [kHz]	ξ_{C3} [kHz]	ξ_{C4} [kHz]
323[b]	7.321 ± 0.257	3.277 ± 0.193	5.934 ± 0.294	21.1[c]	21.1[c]	20.4[c]
303	5.487 ± 0.146	2.564 ± 0.108	3.669 ± 0.143	21.1[c]	21.1[c]	20.4[c]
293	4.603 ± 0.109	2.188 ± 0.081	2.948 ± 0.104	21.1[c]	21.1[c]	20.4[c]
283	3.822 ± 0.105	1.773 ± 0.077	2.388 ± 0.100	21.1[c]	21.1[c]	20.4[c]
273	3.211 ± 0.081	1.489 ± 0.059	1.803 ± 0.073	21.1[c]	21.1[c]	20.4[c]
263	2.465 ± 0.049	1.168 ± 0.037	1.185 ± 0.043	20.6 ± 0.3	20.6 ± 0.3	19.9 ± 0.3
243	1.377 ± 0.044	0.602 ± 0.034	0.695 ± 0.044	20.8 ± 0.3	20.8 ± 0.3	20.1 ± 0.3
228	0.840 ± 0.036	0.328 ± 0.028	0.388 ± 0.037	21.5 ± 0.2	21.5 ± 0.2	20.7 ± 0.2
213	0.500 ± 0.033	0.130 ± 0.047	0.161 ± 0.035	21.6 ± 0.2	21.6 ± 0.2	20.8 ± 0.2

[a] The dipolar coupling constants in eq 4 are divided by 2π. [b] The relaxation rates at this temperature bear nonnegligible contribution from the spin-rotation mechanism. Therefore, results of this analysis were not taken into account neither when Arrhenius plots were performed, nor when activation energies were calculated. [c] Arithmetic mean from values of appropriate dipolar couplings fitted in temperature range 213−263 K. See text for explanation.

two-dimensional (2D) PASS technique,[37] operating under slow MAS conditions. In this method, the overlapping spinning-sideband manifolds are separated by order. Further details of the 2D PASS sequence can be found elsewhere.[37,38] The elements of the symmetric part of the shielding tensors were extracted by a Herzfeld−Berger analysis[39] of the spinning-sideband intensities using the HBA software package.[40] The analysis yields traceless shielding tensors, which is sufficient for our purposes.

Directions of the principal axes of the ^{13}C CSA tensors cannot be determined using the 2D PASS experiments performed on powder samples. Therefore, they were obtained from quantum-mechanical calculations on the DFT[41] level. Molecular geometry for the calculations was taken from neutron diffraction,[7] the basis sets for carbon and hydrogen were IGLO-II,[42] while the IGLO-III basis was used for the nitrogen atom. The exchange-correlation potential was PW91.[43,44] The CSA tensors for ^{15}N were taken from the paper by Lopez et al.[13]

4. Results and Discussion

The full set of spin−lattice relaxation rates and NOE factors for all carbons, measured at three magnetic fields and nine temperatures, is available in the Supporting Information. Here, we present the results of the analysis of this extensive data set.

The first issue to discuss are the interaction strength parameters. Magnitudes of the principal components of the ^{13}C shielding tensors measured in the powder of DMAN perchlorate are listed in Table 1. They were exploited to determine the interaction strengths, χ, according to eqs 5−7, in order to calculate the contribution of this mechanism to ^{13}C relaxation. The DFT calculated tensors (not shown) agreed in all cases reasonably well (within 15 ppm) with the experimental ones. Each of the nonaxially symmetric tensors was decomposed into two axially symmetric tensors, following the procedure given by Werbelow and Canet.[24,45]

The interaction strengths for the dipolar interactions were calculated from the geometry in the crystal.[7] For the sake of accuracy, we took into account couplings not only to the directly bonded protons but also to remote ones. This is necessary, especially for the nonprotonated carbons 9 and 10, because the dipolar mechanism is much more effective than CSA (cf. coefficients multiplying the spectral densities in eq 1), and long-range dipolar couplings constitute an important relaxation source for these carbon nuclei. Relaxation of the carbons 1 and 8 were excluded from our procedure, because we were not able to describe accurately their dipolar couplings to protons of nearby methyl groups, whose fast local dynamics causes the difficulty. The other carbons are relatively far away from the methyl groups, and the effects of the methyl protons motion can safely be neglected, which allows us to include only approximate average couplings to these protons. Knowing the paramaters of relaxation interactions, we employed a numerical Newton−Raphson routine to iteratively change the rotational diffusion

TABLE 3: Results of the ^{15}N Measurements in Deuterium-labeled DMANH$^+$ Compared to Respective Simulations Performed under Assumption of Slow and Fast Proton Jumps[a]

	experimental	slow jumps	fast jumps
	$T = 303$ K		
$(T_1)^{-1}$ (9.4 T) [s^{-1}]	0.0600	0.0684 (1.14)	0.0545 (0.91)
$(T_1)^{-1}$ (11.7 T) [s^{-1}]	0.0590	0.0686 (1.16)	0.0547 (0.93)
$(T_1)^{-1}$ (14.1 T) [s^{-1}]	0.0582	0.0688 (1.18)	0.0550 (0.95)
ρ_S[b](9.4 T) [s^{-1}]	0.0286	0.0336 (1.17)	0.0266 (0.93)
	$T = 293$ K		
$(T_1)^{-1}$ (9.4 T) [s^{-1}]	0.0727	0.0830 (1.14)	0.0661 (0.91)
$(T_1)^{-1}$ (11.7 T) [s^{-1}]	0.0706	0.0831 (1.18)	0.0663 (0.94)
$(T_1)^{-1}$ (14.1 T) [s^{-1}]	0.0674	0.0832 (1.23)	0.0666 (0.99)
ρ_S (9.4 T) [s^{-1}]	0.0353	0.0407 (1.15)	0.0323 (0.91)
	$T = 283$ K		
$(T_1)^{-1}$ (9.4 T) [s^{-1}]	0.0834	0.1008 (1.21)	0.0803 (0.96)
$(T_1)^{-1}$ (11.7 T) [s^{-1}]	0.0846	0.1007 (1.19)	0.0804 (0.95)
$(T_1)^{-1}$ (14.1 T) [s^{-1}]	0.0852	0.1006 (1.18)	0.0805 (0.94)
ρ_S (9.4 T) [s^{-1}]	0.0395	0.0494 (1.25)	0.0392 (0.99)
	$T = 273$ K		
$(T_1)^{-1}$ (9.4 T) [s^{-1}]	0.0981	0.1252 (1.28)	0.0998 (1.02)
$(T_1)^{-1}$ (11.7 T) [s^{-1}]	0.1004	0.1246 (1.24)	0.0995 (0.99)
$(T_1)^{-1}$ (14.1 T) [s^{-1}]	0.1010	0.1239 (1.23)	0.0992 (0.98)
ρ_S (9.4 T) [s^{-1}]	0.0457	0.0613 (1.34)	0.0486 (1.06)
	$T = 263$ K		
$(T_1)^{-1}$ (9.4 T) [s^{-1}]	0.1239	0.1715 (1.38)	0.1367 (1.10)
$(T_1)^{-1}$ (11.7 T) [s^{-1}]	0.1233	0.1689 (1.37)	0.1349 (1.09)
$(T_1)^{-1}$ (14.1 T) [s^{-1}]	0.1221	0.1662 (1.36)	0.1330 (1.09)
ρ_S (9.4 T) [s^{-1}]	0.0586	0.0835 (1.42)	0.0663 (1.13)
	$T = 243$ K		
$(T_1)^{-1}$ (9.4 T) [s^{-1}]	0.1897	0.2801 (1.48)	0.2234 (1.18)
$(T_1)^{-1}$ (11.7 T) [s^{-1}]	0.1892	0.2679 (1.42)	0.2141 (1.13)
$(T_1)^{-1}$ (14.1 T) [s^{-1}]	0.1945	0.2560 (1.32)	0.2052 (1.05)
ρ_S (9.4 T) [s^{-1}]	0.0907	0.1333 (1.47)	0.1058 (1.17)
	$T = 228$ K		
$(T_1)^{-1}$ (9.4 T) [s^{-1}]	0.2904	0.4095 (1.41)	0.3270 (1.13)
$(T_1)^{-1}$ (11.7 T) [s^{-1}]	0.2705	0.3756 (1.39)	0.3010 (1.11)
$(T_1)^{-1}$ (14.1 T) [s^{-1}]	0.2663	0.3475 (1.30)	0.2797 (1.05)
ρ_S (9.4 T) [s^{-1}]	0.1237	0.1812 (1.46)	0.1439 (1.16)
	$T = 213$ K		
$(T_1)^{-1}$ (9.4 T) [s^{-1}]	0.4549	0.5773 (1.27)	0.4632 (1.02)
$(T_1)^{-1}$ (11.7 T) [s^{-1}]	0.3818	0.5170 (1.35)	0.4167 (1.09)
$(T_1)^{-1}$ (14.1 T) [s^{-1}]	0.3423	0.4750 (1.39)	0.3847 (1.12)
ρ_S (9.4 T) [s^{-1}]	0.1410	0.1916 (1.36)	0.1527 (1.08)

[a] Ratios of the calculated to experimental values are given in brackets. [b] The cross-relaxation rate, ρ_S, is obtained from NOE, η, by the relation ρ_S $(\eta\gamma_S)/(T_{1S}\gamma_I)$.

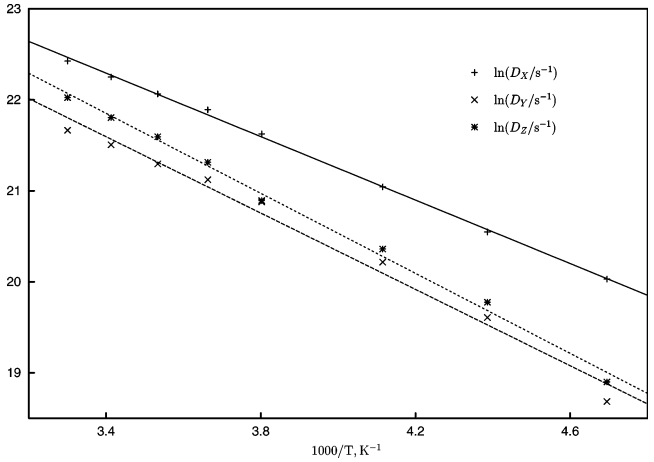

Figure 2. Arrhenius plot for components of the rotational diffusion tensor of $DMANH^+$. The activation energies extracted form the slopes of these lines are 14.5 ± 0.2, 17.4 ± 0.8, and 18.3 ± 0.5 kJ/mol for tumbling about *X*, *Y*, and *Z* axes, respectively.

tensor components of $DMANH^+$ in order to fit the ^{13}C T_1 and NOE data, separately at each temperature of interest. In this procedure, we had to include somehow the vibrational corrections of the dipolar couplings.[23] We did this only for one-bond couplings. Different procedures were used in the low temperature range and at higher temperatures. At low temperatures, where the data are clearly outside of the extreme narrowing regime, we treated one of the directly bonded dipolar couplings as a fitted variable, while ratios of the others to the fitted one were fixed at the values calculated from the solid-state geometry. At high temperatures, we used fixed values of the vibrationally corrected one-bond dipolar coupling, obtained by taking average values over the low-temperature results. Table 2 contains results delivered by this procedure, while Figure 2 shows Arrhenius plots for D_X, D_Y, and D_Z. The fitted dipolar couplings are somewhat lower than the value of about 23 kHz often reported in the solid state for aromatic compounds.[46,47] One should note that the relative standard errors of the estimated diffusion tensor components grow rapidly at temperatures 228 and 213 K. This happens because the carbon longitudinal relaxation is there in the flat region in the vicinity of the T_1 minimum, so that even large changes in molecular reorientation rates have diminished impact on the measured T_1's, compared to higher temperatures. The accuracy of the dipolar coupling estimation is, on the other hand, much better at lower temperatures. The explanation lies in the fact that at higher temperatures ^{13}C relaxation approaches extreme narrowing. Before leaving the carbon relaxation, we wish to comment on the relative importance of the DD and CSA mechanisms for the aromatic carbons in protonated DMAN. The percentage shares of the dipolar terms according to the analysis above in the total spin−lattice relaxation rates are listed in the Supporting Information, together with the experimental data. Here, we state only that the dipolar relaxation is dominant for the proton-bearing carbons, where the dipolar rates constitute between 66 and 91% of the total rates. For the quaternary carbons 9 and 10, the DD contributions are less important, ranging between 4 and 29% and reaching a maximum at the lowest field and temperature of 263 K.

To investigate the bridging proton behavior we decided to exploit ^{15}N longitudinal relaxation and cross-relaxation as probes. Selective substitution of the ^2H isotope instead of ^1H in the methyl groups of $DMANH^+$ diminished significantly the contribution of dipolar relaxation with other nuclei than the bridging proton itself, rendering the dipolar coupling to the latter one the main relaxation mechanism for ^{15}N. However, such a substitution changes the mass distribution of the $DMANH^+$ molecule, which results in a peril that regular $DMANH^+$ and its deuterium-labeled form have different rotational diffusion tensors under the same experimental conditions. To exclude such a possibility we decided to perform ^{13}C T_1 measurements at two temperatures on a sample of the deuterium-labeled form. Since the results were practically identical to those of regular $DMANH^+$, we assume that we can safely interchange the information about the dynamics between both molecules.

The results of ^{15}N measurements for $DMANH^+$ are shown in Table 3, while they are visualized in Figure 3. The results of

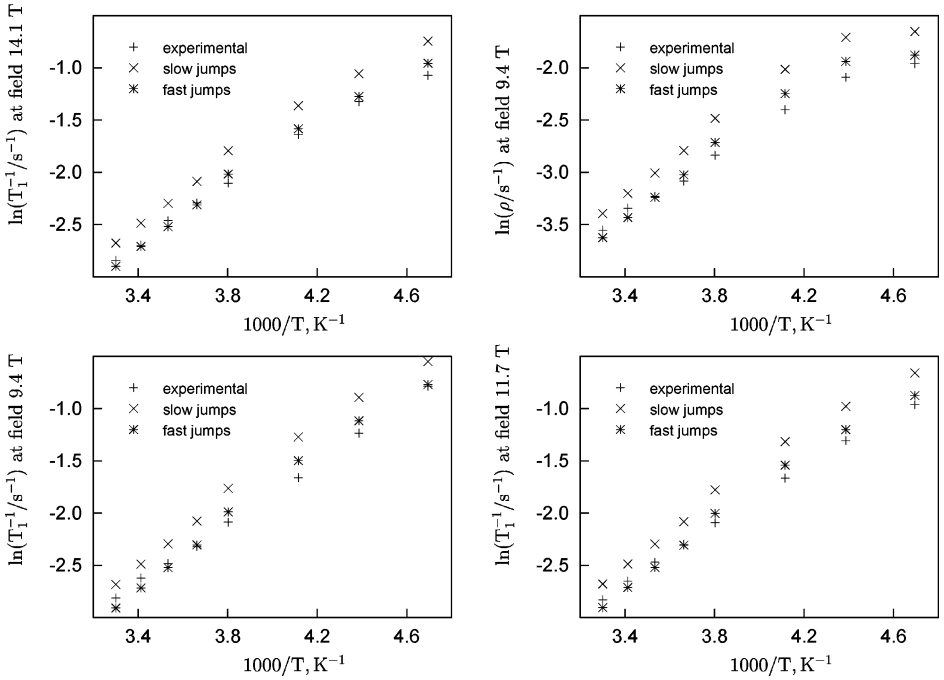

Figure 3. Visualization of ^{15}N longitudinal relaxation data obtained at fields of 9.4, 11.7, and 14.1 T, and cross-relaxation data taken at 9.4 T. For numerical values c.f. Table 3.

simulations within frames of rapid and slow proton jump approximations (eqs 14 and 15) are inserted nearby the experimental values. The simulations were performed under assumptions that the proton bridge geometry obtained from neutron diffraction (N−H distances 1.106 and 1.608 Å, the N−N distance 2.644 Å and N−N−H angles 15.7° and 10.7°, respectively[7]) is conserved also in solution. For the sake of accuracy, the contribution from the CSA mechanism and long-range dipolar couplings were also taken into account. The contributions from the CSA mechanism constitute between 2 and 8% of the measured rates, while the DD interaction with aromatic protons and methyl deuterons contribute about 2−3%. Analysis of the data leads to the conclusion that the model of rapid jumps remains in much better agreement with experimental results than the model of slow jumps. It means that $\lambda_i \gg \lambda_m$, which implies $\lambda_i \geq 10^{10}$ s^{-1}. Attempts of iterative fitting of λ_i were also performed, but failed, probably because of the negligible sensivity of relaxation rates to this parameter in the regime of very fast jumps. Therefore, the obtained "best fit" values bore extremely large standard errors and are not shown.

Such a high proton jump rate is similar to the value determined by Jenkinson et al.[48] for dimers of benzoic acid in the solid state. Since the proton transfer in the latter system involves a tunneling mechanism,[49] we conclude that our result does not exclude such a mechanism also in the present case.

Finally, we would like to note that the rotational diffusion tensor of $DMANH^+$ may be dependent on sample concentration, kind of counteranion, and solvent. We believe, however, that our semiquantitative conclusions concerning the dynamics of proton jumps remain valid also under changes of these experimental conditions.

5. Conclusions

The rotational diffusion tensor of protonated *N*,*N*,*N*′,*N*′-tetramethyl-1,8-naphthalenediamine (DMAN) in isotropic solution was estimated over a wide range of temperatures, by use of ^{13}C NMR relaxation methods. The accuracy of this estimation was very high within, as well as outside, the extreme narrowing regime, while it was slightly worse (but still acceptable) near the ^{13}C T_1 minimum. To the best of our knowledge, this is the first study where a totally anisotropic rotational diffusion was successfully investigated with high accuracy outside of the extreme narrowing regime.

New expressions for relaxation rates in systems involving anisotropic reorientation, accompanied by two-site internal dynamics, were applied for the analysis of ^{15}N relaxation in $DMANH^+$. The analysis showed that proton jumps within the double-well shaped potential are much faster than the molecular reorientation. This is, again to the best of our knowledge, the first case where ultrafast proton jumps were successfully investigated by NMR methods in isotropic liquids.

Acknowledgment. This work was supported by the Swedish Research Council, the Carl Trygger Foundation, and the Magn. Bergvall Foundation. We gratefully acknowledge stimulating discussions with S. Szymański. His generous help in the course of writing this paper was invaluable.

Supporting Information Available: Experimental and calculated ^{13}C relaxation rates. This material is available free of charge via the Internet at http://pubs.acs.org.

References and Notes

(1) Alder, R.; Bowman, P. S.; Steele, W. R. S.; Winterman, D. R. *J. Chem. Soc., Chem. Commun.* **1968**, 723.
(2) Hibbert, F. *J. Chem. Soc., Perkin Trans. 2* **1974**, 1862.
(3) Alder, R. *Chem. Rev.* **1989**, *89*, 1215.
(4) Frey, P. A. *Magn. Reson. Chem.* **2001**, *39*, S190.
(5) Peräkylä, M. *J. Org. Chem.* **1996**, *61*, 7420.
(6) Mallinson, P. R.; Woźniak, K.; Wilson, C. C.; McCormack, K. L.; Yufit, D. S. *J. Am. Chem. Soc.* **1999**, *121*, 4640.
(7) Woźniak, K.; Wilson, C. C.; Knight, K. S.; Jones, W.; Grech, E. *Acta Crystallogr.* **1996**, *B52*, 691.
(8) Pietrzak, M.; Wehling, J.; Limbach, H. H.; Golubev, N. S.; López, C.; Claramunt, R. M.; Elguero, J. *J. Am. Chem. Soc.* **2001**, *123*, 4338.
(9) Grech, E.; Stefaniak, L.; Ando, I.; Yoshimizu, H.; Webb, G. A.; Sobczyk, L. *Bull. Chem. Soc. Jpn.* **1990**, *63*, 2716.
(10) Grech, E.; Stefaniak, L.; Ando, I.; Yoshimizu, H.; Webb, G. A. *Bull. Chem. Soc. Jpn.* **1991**, *64*, 3761.
(11) Gunnarsson, G.; Wennerström, H.; Egan, W.; Forsén S. *Chem. Phys. Lett.* **1976**, *38*, 96.
(12) Altman, L. J.; Laungani, D.; Gunnarsson, G.; Wennerström, H.; Forsén S. *J. Am. Chem. Soc.* **1978**, *100*, 8264.
(13) López, C.; Lorente, P.; Claramunt, R. M.; Marin, J.; Foces-Foces, C.; Llamas-Saiz A. L.; Elguero, J.; Limbach, H.-H. *Ber. Bunsen-Ges. Phys. Chem.* **1998**, *102*, 414.
(14) Langer, U.; Latanowicz, L.; Hoelger, C.; Buntkowsky, G.; Vieth, H.-M.; Limbach, H.-H. *Phys. Chem. Chem. Phys.* **2001**, *3*, 1446.
(15) Hoelger, C.-G.; Wehrle, B.; Benedict, H.; Limbach, H.-H. *J. Phys. Chem.* **1994**, *98*, 843.
(16) Huntress, W. T. *Adv. Magn. Reson.* **1970**, *4*, 1.
(17) Berger, S.; Kreissl, F. R.; Grant, D. M.; Roberts, J. D. *J. Am. Chem. Soc.* **1975**, *97*, 1805.
(18) Levy, G. C.; Craik, D. J.; Norden, B.; Phan Viet, M. T.; Dekmezian, A. *J. Am. Chem. Soc.* **1982**, *104*, 25.
(19) Dölle, A.; Bluhm, Th. *Prog. NMR Spectrosc.* **1989**, *21*, 175.
(20) Wang, D.; Xu, X.; Deng, N.; Pen, L.; Zhang, W.; Stark, R. E. *Magn. Reson. Chem.* **1995**, *33*, 342.
(21) Canet, D. *Nuclear Magnetic Resonance. Concepts and Methods.*; Wiley: Chichester, 1996, Chapter 4.
(22) Kowalewski, J.; Effemey, M.; Jokisaari, J. *J. Magn. Reson.* **2002**, *157*, 171.
(23) Henry, E. R.; Szabo, A. *J. Chem. Phys.* **1985**, *82*, 4753.
(24) Canet, D. *Concepts Magn. Reson.* **1998**, *10*, 291.
(25) Dölle, A.; Suhm, M. A.; Weingärtner, H. *J. Chem. Phys.* **1991**, *94*, 3361.
(26) Hubbard, P. S. *J. Chem. Phys.* **1970**, *52*, 563.
(27) Brüschweiler, R.; Roux, B.; Blackledge, M.; Griesinger, C.; Karplus, M.; Ernst, R. R. *J. Am. Chem. Soc.* **1992**, *114*, 2289.
(28) Woessner, D. E.; Snowden, B. S., Jr.; Meyer, G. H. *J. Chem. Phys.* **1969**, *50*, 719.
(29) Tropp, J. *J. Chem. Phys.* **1980**, *72*, 6035.
(30) Latanowicz, L. *Ber. Bunsen-Ges. Phys. Chem.* **1987**, *91*, 237.
(31) Quast, H.; Risler, W.; Döllscher, G. *Synthesis* **1972**, 558.
(32) Canet, D.; Levy, G. C.; Peat, I. R. *J. Magn. Reson.* **1975**, *18*, 199.
(33) Skelton, N. J.; Palmer, A. G., III; Akke, M.; Kördel, J.; Rance, M.; Chazin, W. J. *J. Magn. Reson.* **1993**, *102*, 253.
(34) Van Geet, A. L. *Anal. Chem.* **1970**, *42*, 679.
(35) Van Geet, A. L. *Anal. Chem.* **1968**, *40*, 2227.
(36) Loening, N. M.; Keeler, J. *J. Magn. Reson.* **2002**, *159*, 55.
(37) Antzutkin, O. N.; Shekar, S. C.; Levitt, M. H. *J. Magn. Reson. A* **1995**, *115*, 7.
(38) Antzutkin, O. N. *Solid-State NMR Spectroscopy: Principles and Applications*; Duer, M. J., Ed.; Blackwell Science: Oxford, 2002.
(39) Herzfeld, J.; Berger, A. E. *J. Chem. Phys.* **1980**, *73*, 6021.
(40) Eichle, K.; Wasylishen, R. E. *HBA: Herzfeld-Berger Analysis Program (version 1.4)*; Dalhousie University: Halifax, Canada, 2001.
(41) deMon Program: Malkin, V. G.; Malkina, O. L.; Casida, M. E.; Salahub, D. R. *J. Am. Chem. Soc.* **1994**, *116*, 5898.
(42) Kutzelnigg, W.; Fleischer, U.; Schindler, M. In *NMR − Basic Principles and Progress*; Diehl, P., Fluck, E.; Günther, H., Kosfeld, R.. Seelig, J., Eds.; Springer: Heidelberg, Germany, 1990; Vol. 23, 165 ff.
(43) Perdew, J. P.; Chevary, J. A.; Vosko, S. H.; Jackson, K. A.; Pederson, M. R.; Singh, D. J.; Fiolhais; C. *Phys. Rev. B* **1992**, *46*, 6671.
(44) Perdew, J. P.; Wang, Y. *Phys. Rev. B* **1992**, *45*, 13244.
(45) Werbelow, L. In *Nuclear Magnetic Resonance Probes of Molecular Dynamics*; Tycko, R., Ed.; Kluwer Academic: Dodrecht, 1994, Chapter 5.
(46) Widmalm, G.; Jansson, K.; Pellijeff, G.; Sandström; D. *J. Phys. Chem. B* **2003**, *107*, 11794.
(47) Hong, M.; Yao, X.; Jakes, K.; Huster, D. *J. Phys. Chem. B* **2002**, *106*, 7355.
(48) Jenkinson, R. I.; Ikram, A.; Horsewill, A. J.; Trommsdorff, H. P. *Chem. Phys.* **2003**, *294*, 95.
(49) Meyer, R.; Ernst, R. R. *J. Chem. Phys.* **1990**, *93*, 5518.